

Testing Cold Dark Matter with the hierarchical buildup of stellar light

Michael L. Balogh¹, Ian G. McCarthy², Richard G. Bower², Vincent R. Eke²

¹*Department of Physics and Astronomy, University of Waterloo, Waterloo, Ontario, N2L 3G1, Canada*

²*Department of Physics, University of Durham, Durham, UK, DH1 3LE*

9 February 2022

ABSTRACT

The hierarchical growth of mass in the Universe is a pillar of all cold dark matter (CDM) models. In this paper we demonstrate that this principle leads to a robust, falsifiable prediction of the stellar content of groups and clusters, that is testable with current observations and is relatively insensitive to the details of baryonic physics or cosmological parameters. Since it is difficult to preferentially remove stars from dark-matter dominated systems, when these systems merge the fraction of total mass in stars can only increase (via star formation) or remain constant, relative to the fraction in the combined systems prior to the merger. Therefore, hierarchical models can put strong constraints on the observed correlation between stellar fraction, f_* , and total system mass, M_{500} . In particular, if this relation is fixed and does not evolve with redshift, CDM models predict $b = d \log f_* / d \log M_{500} \gtrsim -0.3$. This constraint can be weakened if the f_*-M_{500} relation evolves strongly, but this implies more stars must be formed in situ in groups at low redshift. Conservatively requiring that at least half the stars in groups were formed by $z = 1$, the constraint from evolution models is $b \gtrsim -0.35$. Since the most massive clusters ($M \sim 10^{15} M_\odot$) are observed to have $f_* \sim 0.01$, this means that groups with $M = 5 \times 10^{13} M_\odot$ must have $f_* \leq 0.03$. Recent observations by Gonzalez et al. (2007) indicate a much steeper relation, with $f_* > 0.04$ in groups leading to $b \approx -0.64$. If confirmed, this would rule out hierarchical structure formation models: today’s clusters could not have been built from today’s groups, or even from the higher-redshift progenitors of those groups. We perform a careful analysis of these and other data to identify the most important systematic uncertainties in their measurements. Although correlated uncertainties on stellar and total masses might explain the steep observed relation, the data are only consistent with theory if the observed group masses are systematically underestimated.

Key words: galaxies: formation

1 INTRODUCTION

An inescapable prediction of all cold dark matter (CDM) models is that mass in the Universe, in the form of CDM dominated “haloes”, builds up *hierarchically*, with low-mass systems merging to form progressively more massive galaxies and clusters of galaxies (e.g. Bardeen et al. 1986; Davis et al. 1985). Moreover, the rate of this mass growth is precisely determined for a given set of cosmological parameters (e.g. Gao & White 2007). In practice, the complex and non-linear nature of baryonic physics (particularly cooling and heating processes, White & Rees 1978; White & Frenk 1991; Cole et al. 2000; Bower et al. 2006; Croton et al. 2006, and many others) means that this is a difficult prediction to test through observations of galaxies alone. In fact, observations show that galaxies form in the opposite way, with the most massive systems having their stars in place first (e.g. Cowie et al. 1996; Juneau et al. 2005; Pozzetti et al. 2007). This is not considered a falsification of the cold dark

matter model, because the effect can be qualitatively explained by improving the physical description of baryonic processes in the models (e.g. Croton et al. 2006; Bower et al. 2006), in a way that leaves untouched the prediction of hierarchical growth in the dark matter component.

However, an interesting and robust test of the theory can be obtained from observations of the stellar fraction of dark-matter dominated structures. Unlike gas, it is very difficult to separate stars from dark matter, since they are both collisionless forms of matter that interact only via gravity. And while new stars can be formed from gas (a process which is very poorly understood) they can only be destroyed through normal stellar evolution processes (which are quite well understood). The latter effect only removes 10-30 per cent of the total stellar mass, with this range reflecting a weak dependence on star formation history and initial mass function (e.g. Jungwiert et al. 2001; Bruzual & Charlot 2003). Therefore, when two similar systems merge, the mass fraction in visible stars must

be at least as large as the fraction in the combined system prior to the merger, and the simplest expectation is that f_* will either be constant or increase with total system mass.

Stellar fractions are most reliably measured for galaxy clusters, where the total mass in dark matter can be determined in various, independent ways (e.g. gravitational lensing, X-ray gas, or galaxy dynamics). Interestingly, numerous studies have consistently shown that f_* of clusters and groups *decreases* with increasing mass (e.g. Hradecky et al. 2000; Marinoni & Hudson 2002; Eke et al. 2005; Girardi et al. 2002; Ramella et al. 2004; Lin et al. 2004; Balogh et al. 2007). The usual explanation is that clusters are built not only from groups, but also from the accretion of low mass galaxies, where f_* must be very low to explain the shallow faint-end slope of the luminosity function (e.g. White & Frenk 1991; Marinoni & Hudson 2002). Another possibility is that low-mass groups form a significant number of stars, but only *after* most clusters have been assembled. Either possibility allows theory to accommodate a mildly decreasing f_* on cluster scales; it is our goal in this paper to use conservative constraints on these effects to put a robust limit on just how steep this decrease can be.

An important omission in many of the observational studies above, however, has been the contribution from intracluster light (ICL), a low-surface brightness distribution of stars in groups and clusters that is very difficult to measure. Most studies of rich clusters find that the ICL contribution is relatively small, contributing less than 30 per cent to the total stellar light (e.g. Durrell et al. 2002; Feldmeier et al. 2004; Covone et al. 2006; Krick & Bernstein 2007), with at most a weak dependence on system mass (Zibetti et al. 2005). Recently, using deep I -band observations of 23 nearby systems, Gonzalez et al. (2005) have made careful measurements of the ICL component, and come to the surprising conclusion that both f_* and the relative ICL contribution depends much more strongly on mass than has been found previously, with the ICL actually dominating the total stellar mass in groups (Gonzalez et al. 2007, hereafter GZZ). This has motivated us to consider whether or not these observations are able to falsify the hierarchical structure growth model.

We will begin by reanalyzing the observational data of GZZ, and complementary data from Lin & Mohr (2004) in § 2. In § 3 we use theoretical predictions for the growth of dark matter structure to put robust, falsifiable limits on the mass-dependence of f_* . This prediction is then directly confronted with the observational data in § 4, where we also discuss the implications of our findings, and the effect of possible biases and uncertainties in the measurements. Throughout this paper we generally assume a cosmology with $\Omega_m = 0.3$, $\Omega_\Lambda = 0.7$, and $H_0 = 70 \text{ km s}^{-1}$. However we explicitly consider how our results depend on cosmological parameters, in § 3.6.

2 THE STELLAR FRACTION IN LOCAL CLUSTERS AND GROUPS

2.1 Description of the data

We require an accurate account of the relative stellar content for a fair sample of galaxy clusters and groups. We will take most of our data from two of the best recent surveys, GZZ and Lin & Mohr (2004), which are generally complementary in their sources of systematic uncertainty.

GZZ have measured the total light in galaxies and intracluster light, for 23 nearby clusters and groups. They use drift-scan

observations with careful attention to flat-fielding, and fit a two-component de Vaucouleurs (1961) profile to the brightest cluster galaxy (BCG). The outer component, with scale lengths of typically a few hundred kpc, is interpreted as the ICL. Stellar masses are obtained from the integrated I -band luminosity, assuming a mass-to-light ratio of $M/L_I = 3.6$, based on dynamically-determined masses for elliptical galaxies (Cappellari et al. 2006). These masses include a small (about 30%) contribution from the dark matter component; thus we adopt a stellar $M/L = 2.8$ for our analysis, in good agreement with stellar population models assuming a Kroupa (2001) initial mass function, as described in Cappellari et al. (2006). The exact value used does not impact our conclusions, which are derived from the trend of the stellar fraction with system mass, rather than the normalization.

For these 23 clusters, the total I -band light from the BCG and ICL are well characterized, though the relative contribution of each cannot be so robustly determined. The measurement of the total galaxy light is made with a statistical subtraction of the foreground and background population. The main statistical uncertainty in these data arises from the total cluster masses, which are estimated from the line-of-sight velocity dispersion of the galaxies, σ . The relationship between velocity dispersion and dynamical mass is sensitive to the total potential shape, and velocity anisotropy. GZZ partially alleviate this uncertainty by employing a calibration between σ and X-ray derived masses, from an independent cluster sample (Vikhlinin et al. 2006). However, this calibration sample is very small (13 clusters), so it is not possible to determine the scatter about the mean relationship. Moreover, the four lowest mass systems in the GZZ sample require extrapolations of this calibrating relationship, and may therefore be the most unreliable.

The second sample we consider is that of Lin, Mohr & Stanford (2004) and Lin & Mohr (2004, hereafter LM), who analyze K -band observations of 93 X-ray selected clusters, using the 2 Micron All Sky Survey (2MASS, Jarrett et al. 2000). This has the advantages that the stellar mass-to-light ratio (M/L) is only weakly dependent on star formation history, and that the total system masses can be determined from the X-ray temperatures. To ensure the stellar masses can be fairly compared with those of GZZ, we choose an average $M/L_K = 0.9$; this is consistent with the value of $M/L_I = 2.8$ adopted for the GZZ data if $I - K = 2.0$, a reasonable number for the early-type galaxies expected to dominate these clusters (e.g. Poggianti 1997; Smail et al. 2001; Kim & Leei 2005; Eisenhardt et al. 2007). The M/L_K we adopt is somewhat higher than the average value used by Lin et al. (2004) but, again, the absolute value is of little consequence for our analysis. We update the total mass estimates in LM using accurate ASCA temperatures available for 63 of their clusters (Horner 2001; Horner et al. 1999). These temperatures are converted into M_{500}^1 using the relation found by Vikhlinin et al. (2006), where M_{500} was determined from *Chandra* resolved surface brightness and temperature profiles. This typically results in a ~ 20 per cent change to the mass, usually in the sense that our new masses are larger. This corresponds to a ~ 6 per cent change to R_{500} ; therefore we must also correct the measurement of total stellar light within this radius. We simply assume the galaxies follow a Navarro et al. (1997) profile, with a scale radius $r_s = R_{500}/3$, and adjust the total stellar light mea-

¹ M_{500} is defined as the total mass within a radius R_{500} , such that the average density within R_{500} is 500 times the critical density at the cluster redshift.

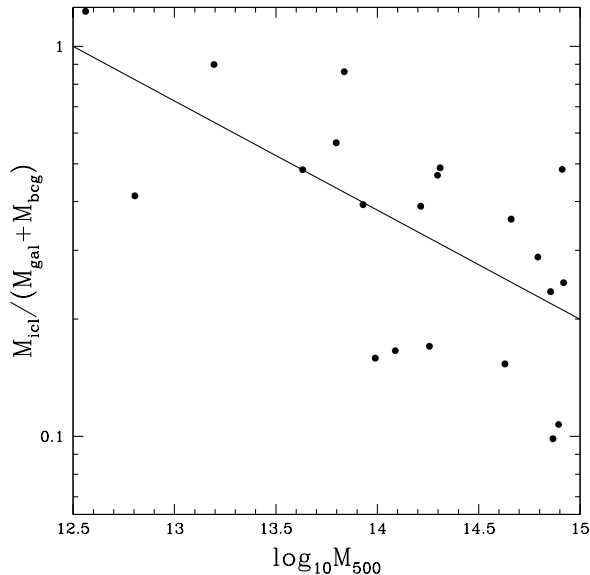


Figure 1. For the cluster sample of Gonzalez et al. (2005), we show the amount of stellar mass in the intracluster light, relative to that in the galaxies (including the BCG), as a function of total mass M_{500} . The solid line shows the relation we adopt to correct the data of LM for the intracluster light component.

sured by LM accordingly. All of these corrections are small, and do not influence our conclusions at all; however, the more precise temperature measurements will result in a more precise mass estimate which, as we discuss in § 2.2, is relevant to our interpretation of the data.

Unfortunately, the infrared data of LM are not deep enough to measure the ICL contribution directly. To make use of these data we need to make an approximate correction for this missing light, and we will use the data of Gonzalez et al. (2005) for this purpose. In Figure 1 we show the mass of the ICL, M_{icl} , relative to the mass in galaxies (including the BCG), as a function of M_{500} . There is a correlation (although largely driven by the four poorly calibrated, lowest-mass systems) and we find approximately

$$\log \left[\frac{M_{icl}}{M_{gal} + M_{bcg}} \right] = -0.28 (\log M_{500} - 12.5), \quad (1)$$

shown as the solid line. That is, for the most massive clusters the ICL contributes another 20% to the mass observed in galaxies, while for the lowest mass systems the total stellar mass is approximately doubled by including the ICL. We will apply this correction to the data of LM. It should be kept in mind that the ICL and BCG light are not robustly separated by Gonzalez et al. (2005), and the BCG light in particular is not measured the same way in both studies. Nonetheless, the correction is not likely to be grossly incorrect, and small differences will not change our main conclusions (see further discussion in § 4.1).

2.2 Correlated Uncertainties

An important consideration in this analysis is proper accounting for uncertainties in the measured quantities. In both GZZ and LM, the statistical uncertainty on $M_{*,500}$ is small, approximately 10 per cent. The dominant statistical uncertainty is in M_{500} , particularly for the GZZ data, where M_{500} is derived from velocity dispersions.

While the number of redshifts per cluster in the GZZ sample is generally more than 20, the uncertainties on σ are still typically $\sim 10\%$, which translates to a $\sim 30\%$ uncertainty on mass, since $M_{500} \propto \sigma^3$. The LM data generally have smaller statistical uncertainties on the masses, partly due to the fact that the mass dependence on temperature ($M_{500} \propto T^{1.5}$) is weaker than on σ .

However, the error analysis is more complex than this because $M_{*,500}$ is the total stellar mass measured within a radius R_{500} , which depends on M_{500} . Therefore, a statistical overestimate of M_{500} will also result in an overestimate of $M_{*,500}$, by an amount that depends on the radial profile of the stellar mass distribution. For the GZZ sample, we use the published radial profile of the BCG and ICL component from Gonzalez et al. (2005). For the galaxy component, we only know the total mass within R_{500} . We will therefore assume the galaxy mass follows a Navarro et al. (1997) profile, with a scale radius $r_s = R_{500}/3$. For each cluster we can then directly calculate $dM_{*,500}/dM_{500}$ and therefore the correlated uncertainty on $M_{*,500}$, $\Delta M_{*,500} = (dM_{*,500}/dM_{500}) \Delta M_{500}$. For the LM data, we do not know the shape of the stellar mass profiles, so we will simply adopt the average value of $dM_{*,500}/dM_{500}$ from the GZZ data; in any case the error bars for these data are generally smaller than the data points in our figures, so this is of no consequence.

2.3 The stellar fraction in the most massive clusters

The most massive clusters are the systems for which all matter is most reliably accounted for observationally. The hot gas is visible as X-ray emission, with a temperature closely related to the gravitational potential, and the total system mass can be directly measured via weak-lensing; both of these methods yield masses in good agreement with those estimated from galaxy velocity dispersions (e.g. Hicks et al. 2006). Moreover, the stellar component is dominated by old, passive galaxies at the present day, so k-corrections and stellar M/L ratios are relatively well determined.

Considering just the most massive systems in GZZ, those with $M_{500} > 3 \times 10^{14} M_{\odot}$, there are eight clusters with stellar fractions ranging from $f_* = 0.006$ to 0.02, and a median of 0.011. In this same mass range, LM find that the fraction of mass in galaxies spans a range of 0.005 to 0.024, with a median of about 0.0095. Including a 20% correction for intracluster light, appropriate for these systems (see § 2), brings the median stellar fraction to 0.011, in excellent agreement with the result of GZZ.

Although these two studies probably provide the most robust measurement of the stellar mass fraction in clusters, the results are consistent with those of many other studies. For example, Eke et al. (2004) find a B -band mass to light ratio of ~ 350 for the most massive systems in the 2dFGRS. Assuming a typical (but very model-dependent) stellar $M/L_B = 4.5$ (Fukugita et al. 1998), this corresponds to a stellar fraction in clusters of 0.013. Girardi et al. (2002) find a higher value of 0.026, assuming the same stellar mass-to-light ratio. Most studies tend to find values between these two; see references within Eke et al. (2004) and Girardi et al. (2002) for a good compilation.

The evidence is therefore good that the stellar fraction in clusters is about 1% on average and certainly $< 3\%$. We note that this is very similar to the global stellar fraction measured from large redshift surveys. Eke et al. (2005) combined the 2dFGRS (Colless et al. 2001) and 2MASS (Jarrett et al. 2000) surveys to find an overall stellar fraction of 0.016 (assuming a Kennicutt 1983, initial mass function), and this is consistent with recent results from many other studies (e.g. Gallazzi et al. 2007, and references within). This small

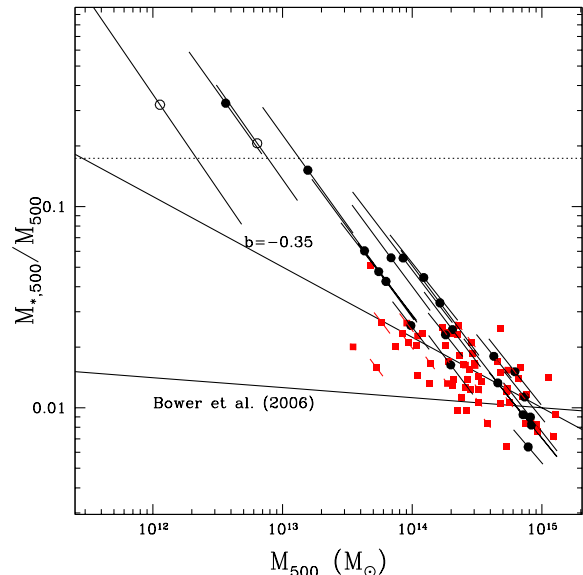


Figure 2. The stellar mass fraction $f_* = M_{*,500}/M_{500}$, including intra-cluster light, is shown as a function of total mass M_{500} . The LM data (red squares) include a correction for ICL estimated from the GZZ data (circles). The two open circles represent clusters A2405 and APMC020, which are systems strongly affected by line-of-sight structure. The 1σ error bars are derived from the published uncertainties on M_{500} , and the tilt reflects the correlated uncertainty in M_{500} and $M_{*,500}/M_{500}$ as described in § 2.2. The horizontal, dotted line shows the global baryon fraction measured by WMAP3 (Spergel et al. 2007). The two solid lines show constant slopes of -0.35 and -0.05 , for comparison with our most conservative theoretical lower limit, and the Bower et al. (2006) model prediction, respectively.

number is already known to put strong constraints on the efficiency of galaxy formation when combined with measurements of the hot gas mass (e.g. Balogh et al. 2001). In § 3 we will show that the stellar fraction alone, independent of how much hot gas may be present, can be used to test models of hierarchical structure formation.

2.4 Observed Mass-Dependence of f_*

We now consider how f_* is observed to depend on system mass. We reproduce the data of LM (including our improved mass estimates and a correction for the ICL contribution) and GZZ² in Figure 2. The error bars represent one standard deviation from the published uncertainties on M_{500} , and we include the correlated uncertainty on $M_{*,500}$ as described in § 2.2. However, in this case the direction of the correlated errors is dominated by the fact that M_{500} appears on both axes.

Both studies find the stellar fraction decreases with increasing cluster mass, in qualitative agreement with other work (e.g. Hradecky et al. 2000; Marinoni & Hudson 2002; Eke et al. 2005; Girardi et al. 2002; Ramella et al. 2004; Balogh et al. 2007). However, it is clear that the slope of the relationship is different, and the

² Note that the four lowest mass systems shown here were excluded from Fig.1 of GZZ, because of uncertainty in the gas mass. However, the gas mass is irrelevant for our purposes, so we include these groups here. Two of the systems, A2405 and APMC020, have two discrete redshift peaks, and A2405 is a clear superposition of two systems.

two datasets are therefore inconsistent for the low-mass systems, with $M \lesssim 2 \times 10^{14} M_\odot$. In fact, GZZ find a remarkably strong trend, with a slope $d \log f_*/d \log M_{500} = -0.64$, such that the least massive systems in their sample have $f_* > 0.17$, in excess of even the total baryon fraction of the Universe (Spergel et al. 2007). Note that the steep trend is not just driven by the last four points, however, and the discrepancy exists even if we ignore these groups. This is a surprising result and, as we will show in the following section, potentially poses a challenge to hierarchical structure growth models.

3 COLD DARK MATTER PREDICTIONS

3.1 The progenitor f_*-M_{500} relation

The data presented in the previous section suggest that f_* decreases with increasing mass, above $M \gtrsim 5 \times 10^{13} M_\odot$. Since CDM theory predicts a robust connection between structures on these scales, we will attempt to secure a prediction for how steep the f_*-M_{500} relationship can be in this regime.

We start by assuming a logarithmic relationship between f_* and M_{500} , for systems with $M > 5 \times 10^{13} M_\odot$, at the present day. We will then attempt to constrain the slope of this relation, $b = d \log f_*/d \log M_{500}$. The model is normalized so that the most massive clusters, with $M_{500} = 10^{15} M_\odot$, have $f_* = 0.01$, as motivated by observations. To be conservative we will assume that haloes with $M < 10^{11} M_\odot$, below the resolution limit of our simulations (described in the following subsection), carry no stars, so $f_* = 0$. For intermediate masses, $10^{11} < M/M_\odot < 5 \times 10^{13}$, where observational constraints are most difficult to acquire, we will adopt three ad-hoc models, which span the full range of realistic behaviour:

(i) **Min:** The stellar fraction is assumed to be constant at a low value of $f_* = 0.01$. This is the most conservative (non-evolving) model, as it will accommodate the steepest slope b while maintaining consistency with a low f_* in massive clusters.

(ii) **Extrap:** The f_*-M_{500} relation is extrapolated to lower masses with the same slope b . However we do not allow it to exceed the universal baryon fraction of 17.5 per cent (Spergel et al. 2007).

(iii) **Mirror:** f_* declines with decreasing mass below $10^{13} M_\odot$, with slope $+|b|$, mirroring the trend at higher masses. Note that since this is a logarithmic slope, $f_* \geq 0.0$ at all masses above our resolution limit.

These three models are shown in Figure 3, with arbitrary slopes (for illustration purposes only) $b = -0.25$, $b = -0.40$ and $b = -0.75$ for the *Min*, *Extrap* and *Mirror* models, respectively. In all cases b refers to the slope for $M > 5 \times 10^{13} M_\odot$, and in practice this slope is a free parameter that we wish to constrain.

These models characterise the $z = 0$ relationship between f_* and mass. This correlation is likely to evolve with redshift, at a rate that depends on the star formation and mass accretion history of haloes at a given mass. We therefore consider a generalized model of f_* :

$$\log f_* = f_o (1+z)^a + b(1+z)^c \log M_{500}, \quad (2)$$

where a and c are free parameters that describe the redshift evolution (in normalization and slope, respectively), and f_o is the normalization of the models at $z = 0$, fixed so that $f_* = 0.013$ at $M_{500} = 7 \times 10^{14} M_\odot$. The present-day slope b is a free parameter for $M > 5 \times 10^{13} M_\odot$; below this mass b behaves as described above for the *Min*, *Extrap* and *Mirror* models.

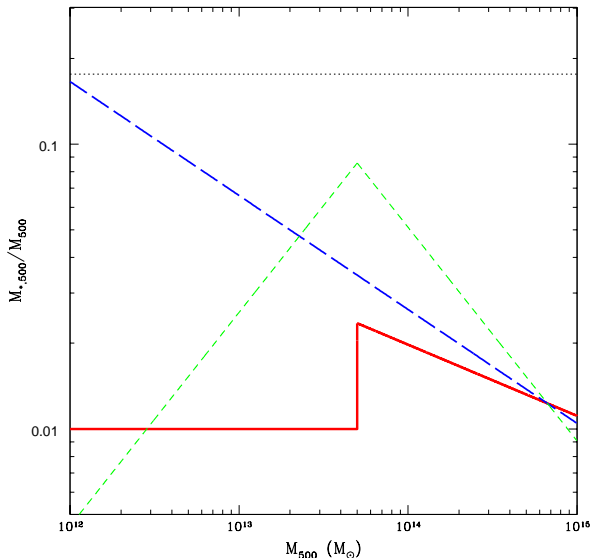


Figure 3. Examples of our three assumed models for the dependence of f_* on halo mass at $z = 0$. For $M > 5 \times 10^{13} M_\odot$, the *Min* model shown here (red, solid line) has a slope of -0.25 , the *Extrap* model (blue, long-dashed line) has a slope of -0.40 , and the *Mirror* model (green, short-dashed line) has a slope of -0.75 . The horizontal, dotted line shows the universal *baryon* fraction from WMAP-3 (Spergel et al. 2007).

3.2 The simulations

We obtain merger trees generated with the *Pinocchio* algorithm (Monaco et al. 2002) to determine the merger history for an ensemble of galaxy clusters. The *Pinocchio* code has been shown to provide results in excellent agreement with full N-body simulations (e.g., it reproduces the mass function of simulated dark matter halos to $\approx 10\%$ accuracy). We have verified this agreement, for a Λ CDM universe, by making an explicit comparison of the predictions of the mean mass growth rate of massive clusters (and the scatter about the mean) with that of clusters of similar mass in the publicly available numerical simulation of Springel et al. (2005). The *Pinocchio* code allows us to efficiently change the mass resolution (to test the sensitivity of the results to this quantity), to increase the simulation box size (in order to generate larger samples of the most massive clusters), and to quickly explore other cosmological models. For all the runs presented in this paper, we adopt a fixed particle mass of $\approx 1.35 \times 10^{10} M_\odot$, which is sufficient to follow the growth of the massive ($> 10^{13} M_\odot$) systems we are interested in. A “resolved” halo corresponds to a system with a minimum of 10 bound particles.

We can then compute the final stellar fraction of a halo of given mass, based on its merger history, by applying each of the models described in § 3.1 to its progenitors. As an example, in Figure 4 we show the evolution of f_* for two massive clusters, using a non-evolving ($a = c = 0$) *Mirror* model (represented as the dashed line) to assign stellar fractions to each merging fragment. Each point represents a merger above our resolution limit. At early times, f_* actually declines, because most of the mass is being accreted below the resolution limit, where we assume conservatively that $f_* = 0$. It is evident from the distance between adjacent points that most of the mass is accreted at late times, in low-mass haloes of $M \approx 1\text{--}10 \times 10^{13} M_\odot$; hence f_* rapidly rises to the corresponding value of ~ 0.03 , and then remains nearly constant at that level. The

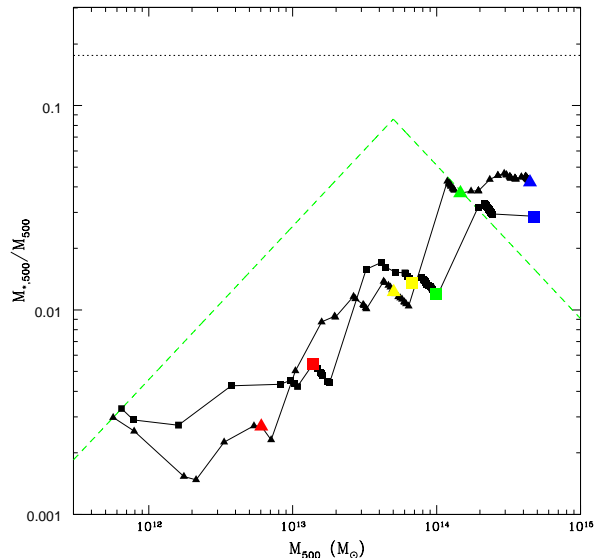


Figure 4. Two examples of the growth history of massive clusters from our Λ CDM *Pinocchio* simulations. Each point (small triangles for one cluster, and small squares for the other) represents a merger event above our mass resolution. The stellar fraction of merging haloes are assumed to follow the *Mirror* model relation shown by the dashed line. For reference, the large red, yellow, green and blue points represent the epochs $z = 2.0, 1.0, 0.5$ and 0 . At early times the cluster is growing primarily from sub-resolution accretion; because we conservatively assume this accretion carries no stars, f_* slowly decreases. However, most of the mass is accreted at late times, through merging with fragments that have $M \sim 10^{13} M_\odot$. Therefore, after $z \sim 1$ f_* quickly increases to ~ 0.03 , and then remains constant at a value *higher* than the dashed line. The cluster that accretes more of its mass from larger progenitors ends up with a lower f_* , as expected.

second cluster trajectory we show is deliberately chosen because it is built from more massive fragments and, as expected, it ends up with a lower final f_* . However, even this cluster has a value of f_* that is a factor of two larger than the assumed *Mirror* model. Therefore this model is internally *inconsistent*: as it is not possible to preferentially remove stars from the final system, we conclude that f_* is too high in the low mass systems (i.e., b is too negative) to be consistent with these being the progenitors of today’s clusters. Since we assume $f_* = 0$ below our resolution limit, increasing the resolution (i.e., lowering the mass limit) serves to increase f_* in the final clusters; apart from this, our results are insensitive to changes in resolution.

3.3 Example: CDM predictions for a non-evolving, steep f_* - M_{500} relation ($b = -0.64$)

To demonstrate how our analysis works, we will consider a non-evolving model with $b = -0.64$, which is the observed $z = 0$ slope as measured from the GZZ data. To be conservative we will adopt the *Min* model prescription for haloes with $M < 5 \times 10^{13} M_\odot$; this gives the best chance of obtaining low f_* in the most massive clusters given a realistic growth history predicted by CDM and a non-evolving f_* - M_{500} relationship. In the following discussion, the *model* refers to the assumed f_* - M_{500} relation that we use to specify the stellar content of the progenitors for a given cluster. The *prediction* refers to the f_* - M_{500} relation that results when a given model is applied to the progenitors of an ensemble of clusters

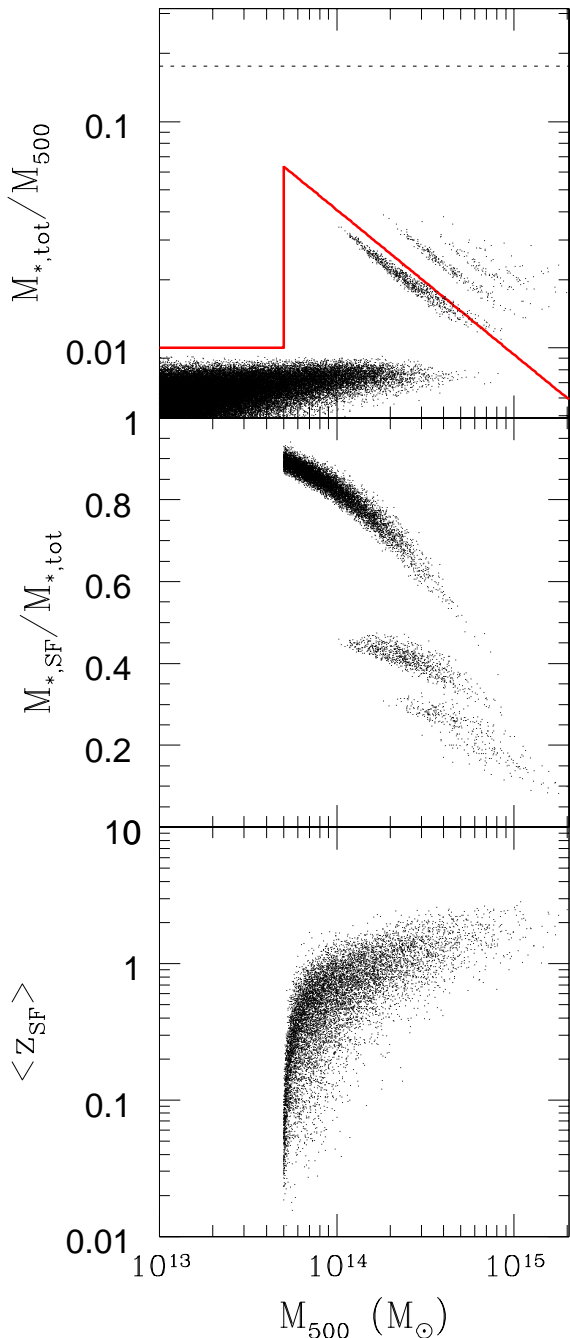


Figure 5. Top: An example of the predicted f_* for an ensemble of clusters in a Λ CDM Universe, assuming a non-evolving *Min* model with $b = -0.64$ (shown as the red, solid line) for the relationship between f_* and M_{500} . The most massive clusters end up with f_* that is much too high, indicating an inconsistent model. In contrast, the lower mass clusters lie *below* the solid line, because they are built from systems with $f_* \lesssim 0.01$. **Middle:** This shows the fraction of stellar mass that has to be added via in situ star formation to keep haloes on the assumed *Min* model (no star formation is invoked if f_* is greater than this). **Bottom:** The average redshift at which stars are added to the halo in situ, as a function of final mass. In this case, we need to add many stars at late times in the lowest mass haloes, to keep f_* as high as 0.05.

with a CDM-specified merger history. Therefore a self-consistent model in the context of CDM is one for which the predicted relation agrees with the model relation.

In the top panel of Figure 5 we show the prediction of the final f_* resulting from this particular model for an ensemble of clusters. The results are somewhat complex, and we see the final clusters are grouped into about six “families”. Let’s consider first the high mass end, $M \gtrsim 5 \times 10^{14}$, where the final clusters follow a slope of $b = -0.64$, like the assumed progenitor model, but with discrete offsets. The majority of these clusters lie nearly on the model line. These are systems which had only one massive ($M > 5 \times 10^{13} M_\odot$) progenitor, which by construction was assumed to have a stellar fraction given by the solid line. A small contribution to the final mass comes from lower mass systems (with $f_* = 0.01$) which is why the clusters lie slightly below the solid line. The next family of points to the right are those clusters that formed from exactly two massive progenitors; thus they have similar values of f_* compared with the first family, but double the final mass. Similarly, the clusters found farther to the right are made from progressively more progenitors with $M > 5 \times 10^{13} M_\odot$. Now considering the whole cluster population, the dominant family is actually comprised of those clusters with $f_* < 0.01$; these are the systems with zero massive progenitors. They have all been built from low mass haloes, including a significant contribution from sub-resolution haloes for which $f_* = 0$.

The predicted f_*-M_{500} correlation is therefore very different from the assumed model (solid line). Since we predict a substantial number of massive clusters with f_* higher than the solid line, this model is internally inconsistent; there is no plausible way to remove stars from the final system, so we can rule this model out without further consideration.

What about the clusters that are predicted to have a *lower* f_* than the assumed model? Unfortunately, these do not represent such a clear failure of the model, since one could always assume that systems form enough stars in situ, *after* a merger event, to move them up to the appropriate value of f_* for their mass³. The middle panel of Figure 5 shows (for clusters with $M > 5 \times 10^{13} M_\odot$) the additional fraction of stars that must be formed in this way to ensure a consistent model. The discontinuity in the model means that clusters just above this threshold must form most of their stars in situ, since their progenitors all have $f_* \leq 0.01$. Moreover, most of this in situ star formation has to occur at late times, since for most of their existence these systems will have had $M < 5 \times 10^{13} M_\odot$, and they have only recently crossed this threshold. We deal with this in the following way. After each merger event, we add sufficient stars, via in situ star formation, to bring the cluster back up to the model (solid line). No stars are added to (or removed from) systems with larger f_* than the model. We can then track the average redshift at which those additional stars were added, and this is shown in the bottom panel of Figure 5. At $M \sim 5 \times 10^{13} M_\odot$, most of the stars must be formed very recently, as argued above. This large amount of recent star formation in groups is not supported by observations, a point on which we will elaborate in § 3.4; so this is another indication that the assumed model is unphysical. For the most massive clusters, we only require that ~ 10 per cent of the stars are formed in situ, and this at $z > 1$, which is much more reasonable.

This fairly complex behaviour nonetheless reflects a consistent trend in most of our models. The hierarchical merging process

³ Note therefore the subtle distinction, that a non-evolving f_*-M_{500} model is not synonymous with a lack of star formation.

always tends to produce final systems with f_* that is *nearly independent of halo mass*. Thus, for models with a steep b , the most massive clusters end up with f_* that is too high (and thus inconsistent), while the least massive end up with f_* that is much too low, and therefore require a lot of recent, in situ star formation. This occurs because the mass accretion histories of clusters over this limited mass range are not very different – they are built from similar-mass haloes over a similar time – resulting in a similar final f_* . Thus we can immediately see from this simple example that CDM will prefer a value of b that is much closer to 0 than the GZZ observations suggest (for non-evolving models).

We have neglected any discussion of the gaseous component of clusters; not only is it dynamically of minor importance, making up < 20 per cent of the cluster mass (e.g. Allen et al. 2004), but it is expected that major mergers are most likely to *remove* gas from the dark matter (e.g. Clowe et al. 2006), and hence further increase f_* . However, it is also possible that low-mass clusters and groups are relatively deficient in gas (e.g. Arnaud & Evrard 1999; Vikhlinin et al. 2006), perhaps because it has been preheated (e.g. Babul et al. 2002; McCarthy et al. 2002); if this gas is accreted later during the hierarchical growth of structure it could cause f_* to decrease. Specifically, if we take the extreme assumption that systems with $M = 10^{13} M_\odot$ have *no* associated gas, then this effect alone would lead only to $b \approx -0.04$, assuming that systems with $M = 10^{15} M_\odot$ have accreted their full complement of gas.

This model also implicitly assumes that the radial distribution of stars traces that of the dark matter and, in particular, is not altered by the merger process. This is a reasonable assumption, as there is no evidence that the stellar fraction is a strong function of radius outside the very centre of clusters, and the stellar light distribution is usually found to be well modelled by a Navarro et al. (1997) profile with a reasonable concentration parameter (e.g. Lin et al. 2004) and comparable to the total mass distribution (Carlberg et al. 1997; Muzzin et al. 2007), even for relatively low mass systems (e.g. Sheldon et al. 2007). Furthermore, while the merging process can greatly distort the relative distribution of gas and dark matter, it is much less likely to separate the stars from the dark matter (e.g. Clowe et al. 2006).

3.4 Constraints

The previous example demonstrates that there are two aspects of our predictions that we can use to choose acceptable models. If many systems end up with f_* greater than assumed in the model, we can confidently rule it out; there is no reasonable way to reduce the number of stars, so the model is internally inconsistent. However, a model could also be deemed unreasonable if it requires that most of the stars are formed too recently. This second constraint is less robust because we require guidance from observations. However, we will show below that we can afford to be quite conservative.

In Figure 6 we show, for a range of evolution parameters a and c , the most negative value of b that yields internally consistent clusters, i.e. those for which the predicted f_* on average lies on or below the assumed f_*-M_{500} model. In principle the evolution could be positive, such that f_* at a given mass scale is greater at high redshift than it is today; for example, if efficient star formation on some scale at $z = 1$ is followed by a long period of quiescent accretion of lower mass haloes, in which star formation has been inefficient. However, in practice, only negative evolution puts interesting constraints on the slope b , so we focus our attention on that regime.

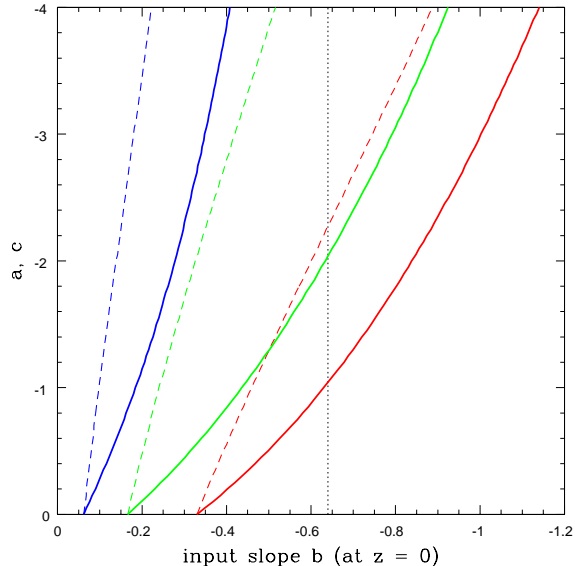


Figure 6. The maximum slope $b = d \log f_* / d \log M_{500}$ at the present day that results in a consistent model with $f_* \leq 0.01$ in the most massive clusters. The line colours correspond to the different models shown in Figure 3, which make different assumptions about the behaviour of f_* for haloes with $M < 5 \times 10^{13} M_\odot$. Dashed lines correspond to evolution in the slope (parameter a in Equation 2) while solid lines represent evolution in the normalization (parameter c). Parameter space to the right of any curve is excluded, as it would lead to clusters with too many stars today. The vertical, dotted line represents the slope measured from the GZZ data.

For each model, represented by a curved line, the region to the right of the plot is excluded. For non-evolving models, $a = c = 0$, all models show $b > -0.33$. This means that, given $f_* = 0.01$ in the most massive clusters, groups with $M \approx 5 \times 10^{13} M_\odot$ must have $f_* < 0.025$. This is considerably shallower than the slope found by GZZ, shown as the vertical, dotted line.

If we allow the $z = 0$ relation to evolve strongly, we can weaken our constraints. This is because the groups that merge to form clusters will have done so at a higher redshift than the groups we are looking at today (recall Figure 4). Figure 6 shows that an arbitrarily steep f_*-M_{500} relation at the present day can be accommodated if it is allowed to evolve strongly enough. However, this success comes at a high price. In hierarchical models, groups with lower mass form at even *higher* redshifts than the clusters, so they will have been built from systems with even lower values of f_* . The natural prediction of these strongly evolving models is therefore that f_* at $z = 0$ will be low not just in clusters, but in *all* haloes. Thus, in order for our model to be consistent, we require that a great deal of stars form in situ in these lower mass haloes, *after* most of the clusters have been assembled, which, for a Λ CDM Universe, is $z \approx 0.3$ (see Figure 9). The more steeply we assume f_* evolves, the more recently those stars must have been created.

We quantify this in Figure 7. For each halo at $z = 0$, we assume that any stars that were generated via in situ star formation formed at the first redshift that any merger yields a stellar fraction below the assumed value⁴. Stars that were accreted through mergers are conservatively assumed to have formed at $z = 2$. We use

⁴ In reality, the stars could form anytime between then and the next merger. This means our results are conservative.

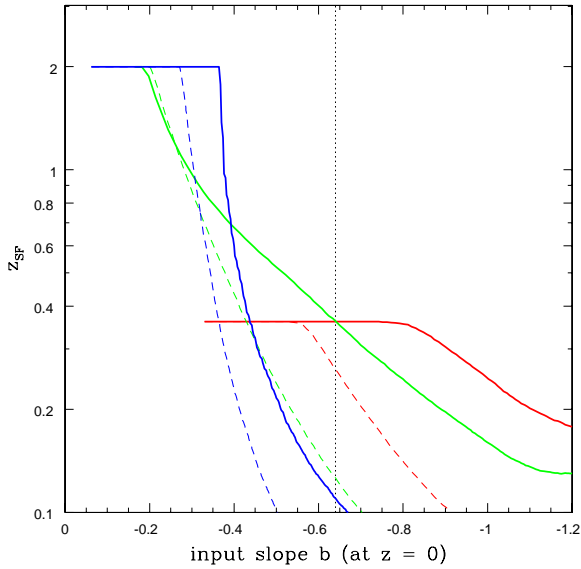


Figure 7. The median redshift at which stars must have formed in haloes with $5 \times 10^{13} < M/M_{\odot} < 10^{14}$, to remain consistent with each model, as a function of the maximum allowable slope b at the present day, from Figure 6. The line styles correspond to those in Figure 6. For each model, more negative values of b imply greater evolution in the f_* - M_{500} relation. The vertical, dotted line represents the slope measured from the GZZ data.

this to compute, for each halo, the redshift at which half the stars were formed in situ, z_{SF} . Figure 7 shows the median z_{SF} for haloes with $5 \times 10^{13} < M/M_{\odot} < 10^{14}$ (i.e. at the low mass end of our models), as a function of the maximum $z = 0$ slope b allowed by each model, from Figure 6. Recall that more negative values of b imply steeper evolution. As described above, the success of strongly-evolving models to match the low f_* in today's clusters comes at the expense of requiring substantial recent star formation in groups.

Although it is clear that galaxy cluster populations are old and passively evolving, with $z_f \gg 2$ (e.g. Bower et al. 1992; De Propris et al. 1999, 2007; Finn et al. 2005; Nelan et al. 2005; Lin et al. 2006; Muzzin et al. 2007), there are fewer constraints on lower mass groups. However, globally we know that the total mass in stars has at most doubled since $z = 1$ (e.g. Dickinson et al. 2003; Bell et al. 2003; Drory et al. 2005; Gwyn & Hartwick 2005; Pozzetti et al. 2007). Relative to the global population, at $z \lesssim 0.5$ groups are known to be dominated by galaxies with early-morphological types and little or no star formation (e.g. de la Rosa et al. 2001; Tran et al. 2001; Balogh et al. 2002, 2004, 2007; Weinmann et al. 2006; Wilman et al. 2005; Jeltama et al. 2007; McGee et al. 2007); therefore we would expect them to have formed half their stars well before $z = 1$. Recently, Brough et al. (2007) have made a detailed analysis of the brightest galaxies (which, together with the ICL, GZZ claim dominate the stellar mass) in three X-ray groups. Two of these have luminosity-weighted ages > 10.5 Gyr (1σ) limit, corresponding to a formation redshift of $z_f = 2$; the youngest has an age limit of > 6.9 Gyr, or $z_f = 0.75$.

We therefore consider that $z_{SF} \gtrsim 1$ (a lookback time of 8 Gyr) is a very reasonable lower limit for the redshift at which groups ($5 \times 10^{13} < M/M_{\odot} < 10^{14}$) have formed most of their stars. From Figure 7 this implies a lower limit of $b > -0.35$, only slightly steeper than the non-evolving model constraints. To accommodate

a slope $b = -0.64$, as observed by GZZ, would require that at least half the stars in groups with $5 \times 10^{13} < M/M_{\odot} < 10^{14}$ formed since $z = 0.35$, which is very unlikely given the above observations.

3.5 Ab-initio models

Instead of assuming a correlation between f_* and M_{500} , an alternative approach is to investigate more complex, ab-initio models that include prescriptions for star formation and feedback. There are many such models currently available, with generally similar recipes (e.g. De Lucia et al. 2006; Croton et al. 2006; Bower et al. 2006). Here we consider the publicly available⁵ predictions of the Bower et al. (2006) model. Figure 8 shows the predicted f_* distribution as a function of halo mass, for all systems in the parent simulation, at redshifts between $z = 0$ and $z = 2$. For halo mass, we use a friends-of-friends mass with linking length $b = 0.2$, which corresponds approximately to M_{200} , with a scatter of about 15 per cent. For a typical cluster halo, $M_{500} \approx 0.65 M_{200}$. There is almost no mass dependence of f_* for $M > 10^{13} M_{\odot}$, and very little evolution in the relation. Above $M = 10^{13} M_{\odot}$, the model at all redshifts satisfies approximately $d \log f_*/d \log M_{500} = -0.05$. This prediction for a nearly constant f_* is also in good agreement with cosmological hydrodynamic simulations that include cooling and feedback physics (e.g. Borgani et al. 2004; Kay et al. 2007), although those simulations tend to predict a higher overall value of f_* .

This prediction for a nearly constant f_* on these scales is not surprising, given that massive groups and clusters are both built from haloes with a similar mass distribution, and over a similar timescale. Although our arguments from the previous section demonstrate that CDM *could* support a f_* - M_{500} relation as steep as $b \approx -0.35$ at the present day, this is only true under the most conservative, and probably unrealistic, assumptions about the value of f_* in haloes with $M_{500} < 5 \times 10^{13} M_{\odot}$ and how this evolves with redshift.

3.6 Other cosmologies

We can hope to put constraints on the cold dark matter model in general, regardless of the specific cosmology, since they are all hierarchical in nature. Different cosmological parameters will result in different rates of formation for haloes of a given mass. We showed in § 3.4 that one can maintain a low f_* in the most massive clusters today, whatever the local f_* - M_{500} relation, as long as this relation evolves strongly with redshift. Clearly one could achieve this same result with weaker evolution, in a cosmology where structure forms earlier. This is true of an open Universe, with $\Omega_m < 1$ and $\Omega_{\Lambda} = 0$ (e.g. van den Bosch 2002); alternatively the epoch of structure formation can be pushed to higher redshift if the normalization of the power spectrum, σ_8 , is increased (e.g. Lacey & Cole 1993). This is illustrated in Figure 9, where we use the Lacey & Cole (1993) model to calculate the probability distribution of the formation redshift, defined as the redshift where 75 per cent of the final mass is in place (see details in Balogh et al. 1999). Distributions are shown for haloes with final masses of $10^{13} M_{\odot}$, $10^{14} M_{\odot}$, and $10^{15} M_{\odot}$, for a range of cosmological parameters. As expected, the highest formation redshifts are obtained in a low- Ω_m or high- σ_8 Universe.

However, in all cases, lower-mass haloes on average form at

⁵ <http://www.icc.dur.ac.uk/>

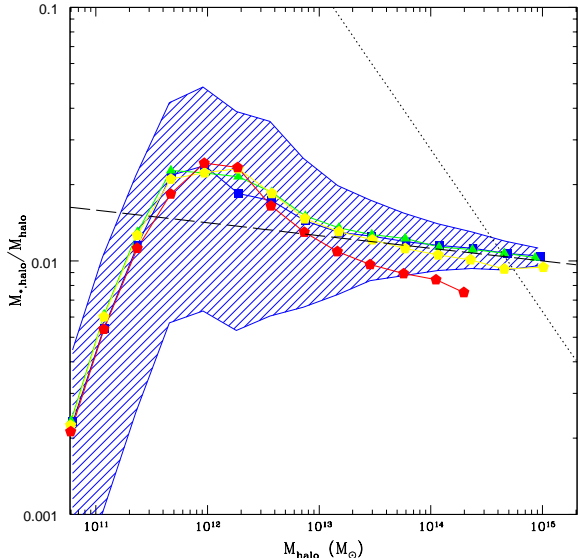


Figure 8. The predicted stellar fraction as a function of halo mass (approximately M_{200}), from the galaxy formation models of Bower et al. (2006). The points represent binned averages at different redshifts: blue, green, yellow, and red points correspond to $z = 0, 0.5, 1.0$, and 2.0 , respectively. The blue shaded region corresponds to the 10th and 90th percentiles of the $z = 0$ distribution. The dashed line is an approximate representation of the $z \leq 1.0$ model data for $M_{500} > 10^{13} M_{\odot}$, and has a slope of $b = -0.05$. The dotted line represents the approximate slope ($b = -0.64$) of the GZZ data, with arbitrary normalization.

even *higher* redshifts; this of course is the well-known behaviour of cold dark matter models. Therefore, in a low- Ω_m or high- σ_8 Universe, galaxy groups had most of their mass in place at even higher redshift than the clusters, and f_* today should also be lower, requiring considerable late-epoch star formation in groups to retain consistency with a steep relation $b \ll 0$. This trade-off means that our constraint on b is unlikely to be changed in different cosmologies.

We have rerun our *Pinocchio* simulations, for an Einstein De-Sitter Universe ($\Omega_m = 1, \Omega_{\Lambda} = 0, \sigma_8 = 0.5$) and an open Universe ($\Omega_m = 0.1, \Omega_{\Lambda} = 0, \sigma_8 = 0.9$). To be conservative we adopt the *Min* model for the f_*-M_{500} relation at $z = 0$, and allow the normalization or slope to evolve rapidly, as $(1+z)^2$. The minimum value of b in this model, that is consistent with $f_* = 0.01$ in the most massive systems and ensures that at least half of the stars formed at $z > 1$, is still $b \approx -0.3$ for the EdS model, but could be relaxed to $b \approx -0.4$ for the Λ CDM cosmology, only slightly steeper than the constraint for our default Λ CDM case. Thus, our conclusions are nearly independent of cosmological parameters, as expected.

4 DISCUSSION

4.1 Observational Uncertainties

As published, the GZZ data show stellar fractions reaching as high as 30% in the lowest mass systems (which, we note, have poorly calibrated M_{500}), well above the WMAP constraints on the global baryon fraction (Spergel et al. 2003, 2007). If this is confirmed to be representative of systems in this mass range, it will rule out hi-

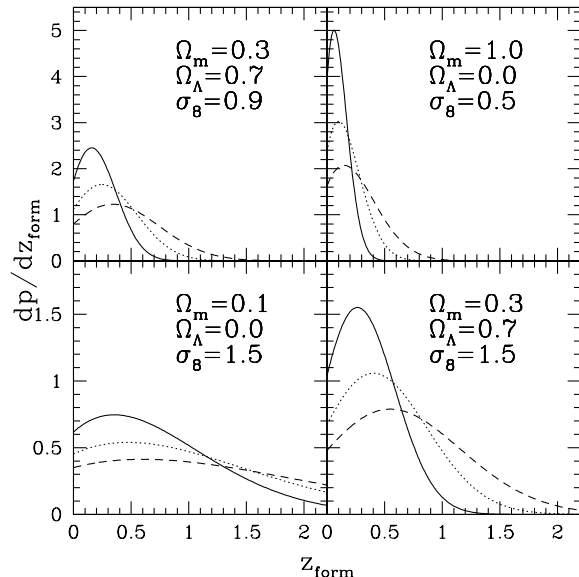


Figure 9. The probability distribution of formation redshifts, defined as the redshift where 75 per cent of the mass is assembled, for clusters with virial masses $M = 10^{15} M_{\odot}$ (solid line), $M = 10^{14} M_{\odot}$ (dotted line), and $M = 10^{13} M_{\odot}$ (dashed line). The calculations are based on the analytic model of Lacey & Cole (1993). Different panels show the results for different cosmological parameters, as indicated. The highest formation redshifts are achieved in low- Ω_m or high- σ_8 models. But in all cases, low-mass haloes form at substantially higher redshift than high-mass haloes. Thus, cosmological parameters have little effect on the generic prediction of hierarchical models, that $b = d \log f_* / d \log M_{500}$ as measured at the present day must be flat, $b > -0.35$.

erarchical structure formation models. The shallower relation between f_* and M_{500} as found by LM, however, does appear to be consistent with such models. In this section we will look carefully at some of the biases and uncertainties involved in the analysis.

One of the most important differences between these two surveys is in the measurement of total mass. GZZ derive masses from the velocity dispersions, which have significant uncertainties themselves, and translate into relative errors three times larger when converted to M_{500} . Moreover, the strong correlation between errors on M_{500} and $M_{*,500}$, as discussed in § 2.2, further complicates matters. To illustrate this better we replot the data in Figure 10, this time showing M_{500} as a function of $M_{*,500}$, so that the tilt in the error bar now reflects the degree of correlation between these two measurements.

It is evident that the error bars have the same “slope” as the GZZ data itself, suggesting that the steepness of their relation is at least partly due to this correlation. However, this may not be the whole story. Accounting for the correlation on the errors, we can compute how likely it would be to find as many systems with $f_* > 0.05$ as GZZ do (seven), if they all actually had $f_* = 0.02$ (consistent with LM), and random uncertainties on σ scatter the observations. This probability is less than 0.1 per cent. The uncertainties on M_{500} do not include the scatter in the $\sigma-M_{500}$ relation from which it is derived; however, even increasing the error bars on σ by 50 per cent, we find that we would only expect to find seven systems with $f_* > 0.05$ six per cent of the time. It is clear from Figure 10 why this is; the GZZ data lie systematically below those of LM; while any one point may be discrepant by only one or two standard deviations, the difference between the two relations

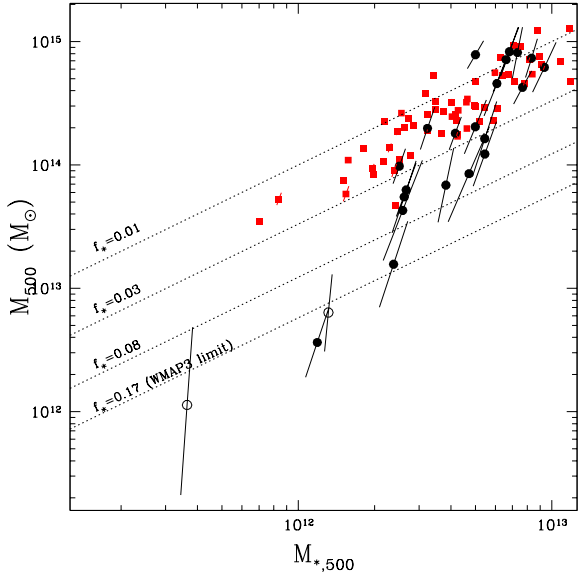


Figure 10. The total mass within R_{500} is shown as a function of the total stellar mass (including intracluster light) within the same radius, for the LM sample (squares) and the GZZ sample (circles). The two open circles represent clusters A2405 and APMC020, which are systems strongly affected by line-of-sight structure. The dashed lines show lines of constant stellar fraction, as indicated. Error bars reflect the uncertainty on M_{500} , and the tilt shows how this is correlated with $M_{*,500}$.

is much more significant. If the source of the discrepancy lies in the total masses, then, it implies that these masses are systematically underestimated for $M_{500} \lesssim 10^{14}$. One possibility is that the velocity dispersions themselves are underestimated; however, this seems unlikely, as several authors have found that σ is quite robust for systems with at least 20 members (e.g. Zabludoff & Mulchaey 1998; Borgani et al. 1999; Hicks et al. 2006). The other, more likely explanation is that the adopted calibration between σ and M_{500} is incorrect at low masses. In particular, the four groups with the lowest σ require an extrapolation of this relationship, which may well be unreliable. Ignoring these four clusters, the remaining GZZ data are statistically consistent with a stellar fraction of 0.02 that is *independent* of cluster mass, and an apparently steep slope that is due entirely to the correlated error bars.

There are other possible sources of systematic error in the data, but none of them seem likely to account for the discrepancy. The most obvious place to look is the intracluster light, since this was not directly measured by LM. In fact, the claim by GZZ that the ICL fraction is such a strong function of mass is not readily apparent in the recent measurements from Zibetti et al. (2005), based on ensemble averages of SDSS clusters. Moreover, numerical simulations generally find that the ICL component should actually be *less* important in groups, relative to clusters (e.g. Murante et al. 2004, 2007). However, even though GZZ claim the ICL doubles the stellar mass in the smallest observed systems, this is still not enough to account for the discrepancy with LM. In Figure 11 we replot the data shown in Figure 10, but excluding the ICL component from both samples. There is still a significant discrepancy between them, and the lowest mass systems in GZZ have stellar fractions $> 10\%$. In particular, if the ICL is ignored, then LM observe a nearly constant f_* over all masses, not only consistent with our theoretical bounds but also in good quantitative agreement with

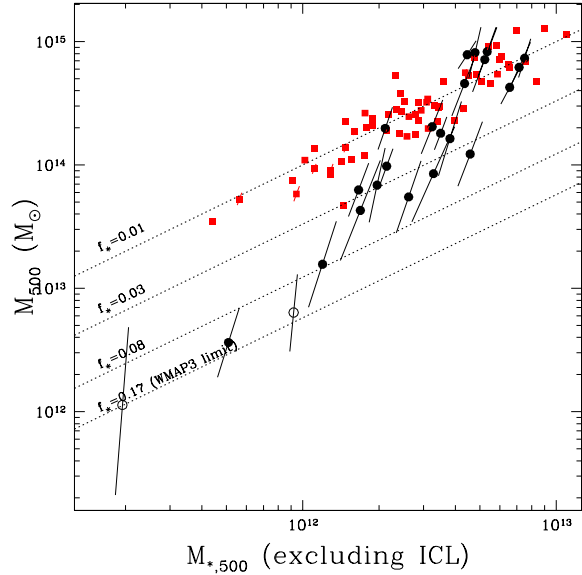


Figure 11. As Figure 10, but where we have excluded the ICL contribution to the stellar light, for both surveys.

ab-initio models (e.g. Bower et al. 2006). On the other hand, GZZ still predict a strong mass dependence of the fractional galaxy light alone.

The dominant systematic uncertainty in the stellar mass measurements are likely in the stellar mass-to-light ratios. The absolute, average, M/L_I adopted is of little consequence, but the relative difference between M/L_I and M/L_K , and any trend in these values with total mass, is relevant. The relative value of M/L_I and M/L_K , and hence the relative normalization of the data in Figs 2, 10 and 11, depends on our assumption that the average galaxy colour is $I - K = 2.0$ in these samples. A bluer population would act to decrease the GZZ stellar masses, relative to LM, and thus decrease the systematic offset observed in these figures. However, no reasonable colour will reconcile the four lowest-mass GZZ groups with those of LM, and the remainder are already consistent with LM (and a constant stellar fraction) given the error bars. Of more interest is the possibility that M/L varies with system mass. If lower-mass clusters have systematically younger stellar populations they will have lower average M/L , and if unaccounted for this would lead to an artificially steep slope b (and would also compromise some of the conclusions in GZZ). However, to explain the discrepancy with the LM data would require that the low-mass clusters of GZZ are systematically bluer than those of LM, while the massive clusters are similar. It seems unlikely that either of these biases are important, since GZZ find that most of the stars in these low-mass systems are in the ICL and BCG component, and the BCG at least is not likely to be much younger than in more massive clusters (e.g. Brough et al. 2007). Moreover, the average stellar M/L in the I band is unlikely to vary by more than a factor of about two, which is insufficient to reconcile the steep slope b observed by GZZ with the model predictions. Nonetheless, deep infrared images of these systems would be very useful.

Another concern might be the contribution to the stellar light from faint, unresolved galaxies; however, both GZZ and LM assume fairly steep, mass-independent faint end slopes when extrapolating the galaxy luminosity function ($\alpha = -1.21$ and $\alpha = -1.1$, respectively), so this cannot contribute to the difference. Finally,

there is a possible selection effect as GZZ select groups to have a dominant galaxy, and this may bias them toward systems with particularly high stellar fractions. Observations of a more representative sample would be valuable, especially if there are sufficient redshifts to robustly identify cluster members. However, in the Bower et al. (2006) models we considered in § 3.5, *none* of the systems in the relevant mass range are found to have stellar fractions as high as even 5%. If these models provide an accurate picture of the local Universe in this respect, then no possible selection bias would lead to the high values of f_* observed by GZZ.

4.2 The consequences

If the strong trend observed by GZZ is confirmed, and found to be typical of a mass-limited sample of groups, what are the theoretical consequences? We have shown that such groups cannot be the progenitors of today's clusters, even if they have built up their high stellar fraction quite recently. One possible implication would be that today's clusters have grown very little in mass since at least $z = 1$, while groups have assembled more recently. This inherently non-hierarchical model would require a lot of suppression of power on group scales; qualitatively this is the behaviour of warm dark matter models, although these generally suppress structure on much smaller scales (e.g. Avila-Reese et al. 2001; Bode et al. 2001). Another possibility is that a large fraction of massive dark matter haloes have *no* stars associated with them, or at least not enough to be detectable. There is some preliminary evidence for such dark clusters (von der Linden et al. 2006; Mahdavi et al. 2007). However, for this to be the solution, the most massive clusters would have to have accreted $\sim 80\%$ of their mass from such objects, while groups still accrete all their mass in haloes with $f_* > 0$. This seems quite unlikely, but should be testable in forthcoming weak-lensing surveys.

On the other hand, if the dynamical masses of the groups in the GZZ sample are underestimated, this raises another theoretical problem. A particularly nice result from GZZ is that (ignoring the four lowest mass clusters) their data give a full account of the baryons: the sum of the stellar mass and the expected gas mass (unfortunately, not directly measured) is comparable to the total baryon fraction in the Universe, and independent of system mass. This is an attractive explanation for the observation that galaxy groups are deficient in X-ray gas (e.g. Arnaud & Evrard 1999; Vikhlinin et al. 2006): the missing gas has cooled to form stars. If GZZ have overestimated f_* , however, this explanation will no longer be viable, and the low gas fractions of groups would likely imply that some powerful form of heating has expelled a large fraction of the gas beyond R_{500} . However, this heating must not be too strong, so that the most massive systems are still able to retain all their gas. This requires something of a delicate balance.

5 CONCLUSIONS

The stellar fraction f_* as a function of cluster mass M_{500} is an important test of hierarchical structure formation models. We find that such models can make a robust, falsifiable prediction that the power-law slope relating these two quantities is $d \log f_* / d \log M_{500} > -0.35$, for systems with $M_{500} > 5 \times 10^{13} M_\odot$. A steeper slope can only be accommodated if the f_* - M_{500} relation evolves strongly, such that galaxy groups formed most of their stars in situ since $z = 1.0$, which is not supported by observations. Since the most massive clusters today (with

$M_{500} \sim 10^{15} M_\odot$) are robustly measured to have $f_* \sim 0.01$, hierarchical models therefore require that galaxy groups (with $M_{500} \sim 5 \times 10^{13} M_\odot$) have $f_* < 0.03$. This constraint is a conservative limit; ab-initio models predict a much flatter relationship with $b > -0.1$ (Bower et al. 2006).

Recent observations by Gonzalez et al. (2007) appear to conflict with this prediction. In particular, their data follow a power-law relation over almost two orders of magnitude in mass, with $b = -0.64$, and the lowest-mass systems in their sample have stellar fractions of 30 per cent, exceeding even the limits on the baryon fraction from WMAP. If confirmed, these observations definitively rule out hierarchical structure formation. *K*-band observations from Lin & Mohr (2004), on the other hand, are just consistent with the model constraints, but may still be inconsistent with the ab-initio model of Bower et al. (2006) if the ICL contribution is as dominant in groups as claimed by Gonzalez et al. (2007). These data do not extend to such low mass systems, nor are their data deep enough to directly measure the important ICL contribution. More observations are needed to resolve the discrepancy between these two studies, and to thereby test the viability of cold dark matter models. Particularly valuable would be X-ray images (and temperature maps) of the Gonzalez et al. (2007) sample, to measure the gas content and total mass, and deep *I* or near-infrared images of the Lin & Mohr (2004) systems to directly measure the ICL component.

We end by noting however that the four lowest-mass systems in the Gonzalez et al. sample have poorly calibrated masses. If we accept that their masses are underestimated by a factor of ten, then the remainder of their data are consistent with a universal stellar fraction of a few percent, and the apparent correlation with system mass is due to the correlated error bars on dynamical and stellar masses. Furthermore, removing these four systems greatly reduces the significance of their claim that the intracluster light fraction is a strong function of mass and, in this case, the Lin & Mohr (2004) data (which have much smaller error bars) are also consistent with a constant stellar fraction $f_* \approx 0.01$. This conclusion challenges the claim by GZZ that the stellar component of galaxy groups is dominated by the BCG and ICL, and that the low gas fractions in these groups is attributable to an increased stellar fraction.

6 ACKNOWLEDGMENTS

We thank the referee, Anthony Gonzalez, for his thorough report, which led to substantial improvements in this paper. This research was supported by the Natural Sciences and Engineering Research Council of Canada, through a Discovery Grant to M. Balogh. IGM acknowledges support from a NSERC Postdoctoral Fellowship, and thanks Tom Theuns for his assistance with the use of the *Pinocchio* software. VRE acknowledges support from the Royal Society for a University Research Fellowship.

REFERENCES

- Allen, S. W., Schmidt, R. W., Ebeling, H., Fabian, A. C., & van Speybroeck, L. 2004, MNRAS, 353, 457
- Arnaud, M. & Evrard, A. E. 1999, MNRAS, 305, 631
- Avila-Reese, V., Colín, P., Valenzuela, O., D'Onghia, E., & Firmani, C. 2001, ApJ, 559, 516
- Babul, A., Balogh, M. L., Lewis, G. F., & Poole, G. B. 2002, MNRAS, 330, 329

- Balogh, M., Bower, R. G., Smail, I., Ziegler, B. L., Davies, R. L., Gaztelu, A., & Fritz, A. 2002, *MNRAS*, 337, 256
- Balogh, M. L., Babul, A., & Patton, D. R. 1999, *MNRAS*, 307, 463
- Balogh, M. L., Pearce, F. R., Bower, R. G., & Kay, S. T. 2001, *MNRAS*, 326, 1228
- Balogh, M. L., Wilman, D., Henderson, R. D. E., Bower, R. G., Gilbank, D., Whitaker, R., Morris, S. L., Hau, G., Mulchaey, J. S., Oemler, A., & Carlberg, R. G. 2007, *MNRAS*, 374, 1169
- Balogh, M. L. et al. 2004, *MNRAS*, 348, 1355
- Bardeen, J. M., Bond, J. R., Kaiser, N., & Szalay, A. S. 1986, *ApJ*, 304, 15
- Bell, E. F., McIntosh, D. H., Katz, N., & Weinberg, M. D. 2003, *ApJS*, 149, 289
- Bode, P., Ostriker, J. P., & Turok, N. 2001, *ApJ*, 556, 93
- Borgani, S., Girardi, M., Carlberg, R. G., Yee, H. K. C., & Ellingson, E. 1999, *ApJ*, 527, 561
- Borgani, S., Murante, G., Springel, V., Diaferio, A., Dolag, K., Moscardini, L., Tormen, G., Tornatore, L., & Tozzi, P. 2004, *MNRAS*, 348, 1078
- Bower, R. G., Benson, A. J., Malbon, R., Helly, J. C., Frenk, C. S., Baugh, C. M., Cole, S., & Lacey, C. G. 2006, *MNRAS*, 370, 645
- Bower, R. G., Lucey, J. R., & Ellis, R. S. 1992, *MNRAS*, 254, 601
- Brough, S., Proctor, R., Forbes, D. A., Couch, W. J., Collins, C. A., Burke, D. J., & Mann, R. G. 2007, *MNRAS*, 378, 1507
- Bruzual, G. & Charlot, S. 2003, *MNRAS*, 344, 1000
- Cappellari, M. et al. 2006, *MNRAS*, 366, 1126
- Carlberg, R. G., Yee, H. K. C., & Ellingson, E. 1997, *ApJ*, 478, 462
- Clowe, D., Bradač, M., Gonzalez, A. H., Markevitch, M., Randall, S. W., Jones, C., & Zaritsky, D. 2006, *ApJL*, 648, L109
- Cole, S., Lacey, C. G., Baugh, C. M., & Frenk, C. S. 2000, *MNRAS*, 319, 168
- Colless, M. et al. 2001, *MNRAS*, 328, 1039
- Covone, G., Adami, C., Durret, F., Kneib, J.-P., Lima Neto, G. B., & Slezak, E. 2006, *A&A*, 460, 381
- Cowie, L. L., Songaila, A., Hu, E. M., & Cohen, J. G. 1996, *AJ*, 112, 839
- Croton, D. J. et al. 2006, *MNRAS*, 365, 11
- Davis, M., Efstathiou, G., Frenk, C. S., & White, S. D. M. 1985, *ApJ*, 292, 371
- de la Rosa, I. G., de Carvalho, R. R., & Zepf, S. E. 2001, *AJ*, 122, 93
- De Lucia, G., Springel, V., White, S. D. M., Croton, D., & Kauffmann, G. 2006, *MNRAS*, 366, 499
- De Propriis, R., Stanford, S. A., Eisenhardt, P. R., Dickinson, M., & Elston, R. 1999, *AJ*, 118, 719
- De Propriis, R., Stanford, S. A., Eisenhardt, P. R., Holden, B. P., & Rosati, P. 2007, *AJ*, 133, 2209
- de Vaucouleurs, G. 1961, *ApJS*, 5, 233
- Dickinson, M., Papovich, C., Ferguson, H. C., & Budavári, T. 2003, *ApJ*, 587, 25
- Drory, N., Salvato, M., Gabasch, A., Bender, R., Hopp, U., Feulner, G., & Pannella, M. 2005, *ApJL*, 619, L131
- Durrell, P. R., Ciardullo, R., Feldmeier, J. J., Jacoby, G. H., & Sigurdsson, S. 2002, *ApJ*, 570, 119
- Eisenhardt, P. R., De Propriis, R., Gonzalez, A. H., Stanford, S. A., Wang, M., & Dickinson, M. 2007, *ApJS*, 169, 225
- Eke, V. R., Baugh, C. M., Cole, S., Frenk, C. S., King, H. M., & Peacock, J. A. 2005, *MNRAS*, 362, 1233
- Eke, V. R. et al. 2004, *MNRAS*, 355, 769
- Feldmeier, J. J., Ciardullo, R., Jacoby, G. H., & Durrell, P. R. 2004, *ApJ*, 615, 196
- Finn, R. A. et al. 2005, *ApJ*, 630, 206
- Fukugita, M., Hogan, C. J., & Peebles, P. J. E. 1998, *ApJ*, 503, 518
- Gallazzi, A., Brinchmann, J., Charlot, S., & White, S. D. M. 2007, *MNRAS*, submitted, astro-ph/0708.0533
- Gao, L. & White, S. D. M. 2007, *MNRAS*, 377, L5
- Girardi, M., Manzato, P., Mezzetti, M., Giuricin, G., & Limboz, F. 2002, *ApJ*, 569, 720
- Gonzalez, A. H., Zaritsky, D., & Zabludoff, A. I. 2005, *ApJ*, 618, 195
- . 2007, *ApJ*, 666, 147
- Gwyn, S. D. J. & Hartwick, F. D. A. 2005, *AJ*, 130, 1337
- Hicks, A. K., Ellingson, E., Hoekstra, H., & Yee, H. K. C. 2006, *ApJ*, 652, 232
- Horner, D. 2001, PhD thesis, University of Maryland
- Horner, D. J., Mushotzky, R. F., & Scharf, C. A. 1999, *ApJ*, 520, 78
- Hradecky, V., Jones, C., Donnelly, R. H., Djorgovski, S. G., Gal, R. R., & Odewahn, S. C. 2000, *ApJ*, 543, 521
- Jarrett, T. H., Chester, T., Cutri, R., Schneider, S., Skrutskie, M., & Huchra, J. P. 2000, *AJ*, 119, 2498
- Jeltema, T. E., Mulchaey, J. S., Lubin, L. M., & Fassnacht, C. D. 2007, *ApJ*, 658, 865
- Juneau, S. et al. 2005, *ApJL*, 619, L135
- Jungwiert, B., Combes, F., & Palouš, J. 2001, *A&A*, 376, 85
- Kay, S. T., da Silva, A. C., Aghanim, N., Blanchard, A., Liddle, A. R., Puget, J.-L., Sadat, R., & Thomas, P. A. 2007, *MNRAS*, 377, 317
- Kennicutt, R. C. 1983, *ApJ*, 272, 54
- Kim, T. & Leei, M. G. 2005, *Journal of Korean Astronomical Society*, 38, 145
- Krick, J. E. & Bernstein, R. A. 2007, *AJ*, 134, 466
- Kroupa, P. 2001, *MNRAS*, 322, 231
- Lacey, C. & Cole, S. 1993, *MNRAS*, 262, 627
- Lin, Y., Mohr, J. J., & Stanford, S. A. 2004, *ApJ*, 610, 745
- Lin, Y.-T. & Mohr, J. 2004, *ApJ*, 617, 879
- Lin, Y.-T., Mohr, J. J., Gonzalez, A. H., & Stanford, S. A. 2006, *ApJL*, 650, L99
- Mahdavi, A., Hoekstra, H., Babul, A., Balam, D. D., & Capak, P. L. 2007, *ApJ*, 668, 806
- Marinoni, C. & Hudson, M. J. 2002, *ApJ*, 569, 101
- McCarthy, I. G., Babul, A., & Balogh, M. L. 2002, *ApJ*, 573, 515
- McGee, S., Balogh, M., Henderson, R. D. E., Wilman, D. J., Bower, R. G., Mulchaey, J. S., & Oemler, A. 2007, *MNRAS*, submitted
- Monaco, P., Theuns, T., & Taffoni, G. 2002, *MNRAS*, 331, 587
- Murante, G., Arnaboldi, M., Gerhard, O., Borgani, S., Cheng, L. M., Diaferio, A., Dolag, K., Moscardini, L., Tormen, G., Tornatore, L., & Tozzi, P. 2004, *ApJL*, 607, L83
- Murante, G., Giovali, M., Gerhard, O., Arnaboldi, M., Borgani, S., & Dolag, K. 2007, *MNRAS*, 377, 2
- Muzzin, A., Yee, H. K. C., Hall, P. B., & Lin, H. 2007, *ApJ*, 663, 150
- Navarro, J. F., Frenk, C. S., & White, S. D. M. 1997, *ApJ*, 490, 493
- Nelan, J. E., Smith, R. J., Hudson, M. J., Wegner, G. A., Lucey, J. R., Moore, S. A. W., Quinney, S. J., & Suntzeff, N. B. 2005, *ApJ*, 632, 137
- Poggianti, B. M. 1997, *A&ASS*, 122, 399
- Pozzetti, L. et al. 2007, *ArXiv e-prints*, 704

- Ramella, M., Boschin, W., Geller, M. J., Mahdavi, A., & Rines, K. 2004, *AJ*, 128, 2022
- Sheldon, E. S. et al. 2007, *ArXiv e-prints*, 709
- Smail, I., Kuntschner, H., Kodama, T., Smith, G. P., Packham, C., Fruchter, A. S., & Hook, R. N. 2001, *MNRAS*, 323, 839
- Spergel, D. N. et al. 2003, *ApJS*, 148, 175
- . 2007, *ApJS*, 170, 377
- Springel, V. et al. 2005, *Nature*, 435, 629
- Tran, K. H., Simard, L., Zabludoff, A. I., & Mulchaey, J. S. 2001, *ApJ*, 549, 172
- van den Bosch, F. C. 2002, *MNRAS*, 331, 98
- Vikhlinin, A., Kravtsov, A., Forman, W., Jones, C., Markevitch, M., Murray, S. S., & Van Speybroeck, L. 2006, *ApJ*, 640, 691
- von der Linden, A., Erben, T., Schneider, P., & Castander, F. J. 2006, *A&A*, 454, 37
- Weinmann, S. M., van den Bosch, F. C., Yang, X., Mo, H. J., Croton, D. J., & Moore, B. 2006, *MNRAS*, 372, 1161
- White, S. D. M. & Frenk, C. S. 1991, *ApJ*, 379, 52
- White, S. D. M. & Rees, M. J. 1978, *MNRAS*, 183, 341
- Wilman, D. J., Balogh, M. L., Bower, R. G., Mulchaey, J. S., Oemler, A., Carlberg, R. G., Morris, S. L., & Whitaker, R. J. 2005, *MNRAS*, 358, 71
- Zabludoff, A. I. & Mulchaey, J. S. 1998, *ApJ*, 496, 39
- Zibetti, S., White, S. D. M., Schneider, D. P., & Brinkmann, J. 2005, *MNRAS*, 358, 949